Chapter 20

Spectral Analysis
Quantifying Variation in Time and Space

In our investigation of variation and its effects on organisms in Chapter 19, we used the variance as our primary metric of variability. But when it comes to characterizing nature's fluctuations, variance is a blunt instrument. For example, in a certain habitat we might find that air temperature fluctuates with a variance of 100° squared, but that bare statistic can't tell us whether that fluctuation happens in minutes, hours, or days. Similarly, prey density might vary by 1000 individuals per hectare, squared, but that variance tells us nothing about the spatial distribution of prey. In order to effectively incorporate the consequences of variation into our understanding of ecomechanics, we need to quantify its temporal and spatial patterns.

To that end, this chapter introduces *spectral analysis*, a basic method for exploring the patterns of variation. Although spectral analysis is a standard statistical tool in physics and engineering, it has escaped the notice of most biologists. I hope that in this and the following chapter I can convince you that it provides a valuable perspective on both life and the physical environment.

As a preview of where we are headed, consider the mystery of the ice ages. Beginning in the mid-1700s, scientists began to notice evidence that at multiple times in the past, ice covered much of the globe: morraines of glacial till far from present-day glaciers, ice-worn boulders where in current times there was no ice. As the evidence mounted, so did the perplexity. What could possibly have caused earth's climate to be so much colder in the past, and why did the episodes reoccur?

A variety of explanations were proposed, but none gained traction until Milutin Milancović (a Serbian mathematician, geophysicist, and astronomer) was interned as a prisoner of war in 1914. Finding himself with time on his hands, he laboriously calculated the dynamics of Earth's rotation and its orbit around the sun, leading him to the conclusion that the amount of solar radiation impinging on Earth—and thereby its temperature—should vary with cycles of approximately 23,000, 41,000, and 100,000 y. Milancović proposed that these celestial oscillations caused Earth's recurrent ice ages.

For decades, Milancović's theory was viewed with skepticism. It didn't help that one of Milancović's most ardent supporters was Alfred Wegener, the German

meteorologist infamous for proposing the (then) absurd idea that continents drifted. But, beginning in the 1960s, paleoclimatologists were able to piece together a record of earth's temperature extending back five million years (Figure 20.1A). Clearly, temperature has varied episodically, but how could one tell from this complex record whether those variations matched the cycles predicted by Milancović?

The answer was spectral analysis. Applying the techniques we will develop in this chapter, climatologists have been able to carefully measure the periodicities of the ice ages, and they indeed match those proposed by Milancović. From 2.5 to 1 million years ago, ice ages occurred on average every 41,000 y, and from 1 million years ago to the present, every 100,000 y. Debate continues over the mechanism by which celestial factors trigger ice ages, but—due to spectral analysis—there is no doubt that the Milancović cycles are real.

Knowing the pattern of ice ages provides potentially useful information for biologists. In the era when ice ages occurred every 41,000 y, the average rate of climatic change was faster than in recent times when the glaciers arrived every 100,000 y. Through study of the fossilized remains of these different eras, paleontologists can perhaps find clues as to how nature will react to the current rapid rate of climate change.

Ocean waves offer another example, one that we will develop in this chapter. Wind blowing across the ocean surface creates waves that, as they approach shore, cause water to flow back and forth over benthic organisms such as corals. The higher the waves, the faster the flow; the longer the wave period, the longer water flows in each direction. Together, these factors govern the rate at which carbon and nutrients are transported across the benthic boundary layer to corals' symbiotic algae. For a given sea state—which comprises a complex pattern of surface oscillation (Figure 20.1B)—how fast are carbon and nutrients delivered? To answer this question, we need information about how wave height varies as a function of wave period, information that spectral analysis can provide.

Milancović cycles and ocean waves vary through time, but spectral analysis is equally useful for quantifying the pattern of variation through space. Desert lizards eat beetles, for instance, and the density of beetles varies through space (a hypothetical example is shown in Figure 20.1C). If a lizard travels 20 m across the desert floor, how much variation in prey density will it encounter on average? How much if it travels 40 m? Again, these are questions that spectral analysis can answer.

1 SEQUENCE, SIGNAL, AND POWER

In each of these cases (Milancović cycles, ocean waves, desert beetles) it is the sequence of the data that distinguishes them from data more commonly encountered in standard inferential statistics. Consider, for instance, our data regarding the density of desert beetles. If we collect 500 measurements of prey density along a lizard's foraging path ($x_1, x_2, \ldots, x_{500}$) we can calculate the mean and variance of density:

$$\overline{x} = \frac{1}{500}\sum_{i=1}^{500} x_i, \tag{20.1}$$

$$\sigma_x^2 = \frac{1}{500}\sum_{i=1}^{500} (x_i - \overline{x})^2. \tag{20.2}$$

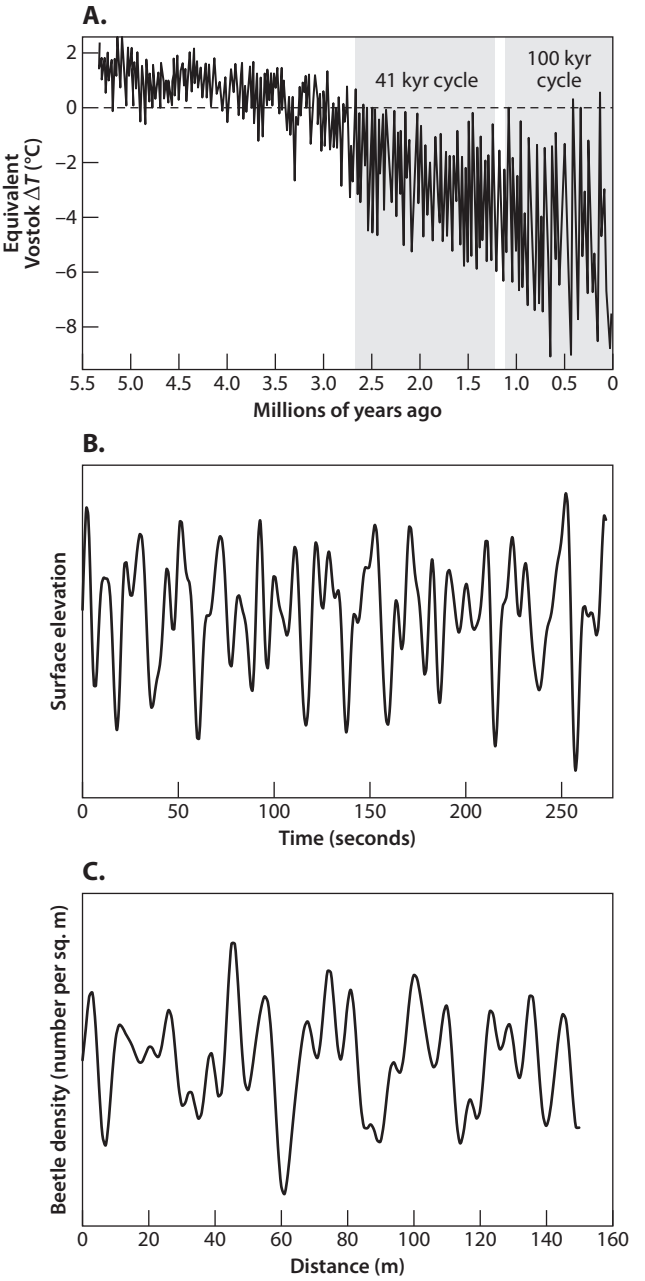

Figure 20.1 The average temperature on Earth has fluctuated for the last five million years (**A**), and the period of oscillation has shifted through time (modified from a figure by R. A. Rohde, Global Warming Art). **B**. A hypothetical temporal record of ocean surface elevation. **C**. A hypothetical record of beetle density as a function of distance along a transect.

The order in which we enter data into these calculations doesn't matter; we could draw the data out of a hat and get the same results. But knowing the data's *sequence* provides information beyond the mean and variance, and sequence is key to the analysis of pattern.

Much of what we know about the analysis of sequential data was first worked out by electrical engineers in the communications industry. As a result, the literature is rife with terms such as *signal* and *power* that have practical meaning when applied to the process of, for instance, getting a telephone conversation from one location to another. However, over the years these terms have been co-opted to apply to situations in which they have little intuitive meaning. Best that we grasp the intent of these terms here at the beginning.

In the context of communications, a *signal* is information conveyed, and quite often the mechanism of conveyance is an electrical voltage. For example, when you talk on the phone, the sound of your voice is converted by a microphone into a varying voltage, and information about this variation is transmitted by wires, optical fibers, or radio waves to another telephone. Upon arrival, the information is transduced back into a voltage signal, which causes a speaker to vibrate around its average position. The resulting sound waves carry your words to the recipient's ear.

Note that it is variation in voltage (rather than voltage itself) that makes the system useful. If the information you transmitted corresponded to a constant voltage, the speaker in the receiving phone would move to a constant position, after which no sound would be produced: no sound, no conveyance of information. Thus, in the context of a telephone conversation, the term signal can be used as an informal synonym for the pattern—the sequence—of deviations from the mean. Signal is often used in this fashion even when the variation being discussed has no association with human communication. For instance, we could easily talk about the wave-height signal of our ocean data or the density signal of our beetles.

If we were to delve deeply into spectral analysis, we would need to differentiate carefully between signal and *noise*. In this context, noise is also used to describe deviations from the mean, but the term is confined to deviations that hinder the conveyance of information. For example, random deviations (which convey no information) can obscure the presence of a signal, and therefore constitute noise. For simplicity, I'll assume in this chapter that all the variation in a data series conveys useful information.

The historical use of the term signal to describe variation in voltage leads naturally to the concept of *power*. Voltage is a measure of the potential energy electrons have for movement, and amperage is a measure of current, the rate at which electrons flow. In an electrical circuit, power—the energy per time it takes to move current—is equal to the voltage V applied to the circuit times the resulting amperage I:

$$\text{electrical power} = VI. \tag{20.3}$$

For example, a typical circuit in your house operates at 120 volts (V) and is capable of safely carrying 20 amperes (A). As a result, you can power a hair dryer that produced $120\ \text{V} \times 20\ \text{A} = 2400\ \text{W}$ of heat.

A second basic relationship (Ohm's law) tells us that the current moving in a circuit is directly proportional to V and inversely proportional to R, the circuit's resistance:

$$I = \frac{V}{R}. \tag{20.4}$$

Inserting this relationship into equation 20.3, we see that electrical power is proportional to the square of voltage:

$$\text{electrical power} = \frac{V^2}{R}. \tag{20.5}$$

Now consider a voltage that varies through time. Some power is expended in association with the average voltage $\overline{V}$, but there is also electrical power expended by the fluctuations of voltage away from the mean (i.e., the power of the signal's alternating-current (AC) component). By measuring voltage at n points in time and combining equations 20.1 and 20.5, we find that the average power of this fluctuating signal is,

$$\text{average AC power} = \frac{1}{Rn}\sum_{i=1}^{n}\left(V_i - \overline{V}\right)^2. \tag{20.6}$$

That is, AC power is proportional to the average squared deviation in voltage. But the average squared deviation is, by definition, the signal's variance (see equation 20.2). In other words, when an electrical engineer calculates the variance in voltage, he or she is implicitly calculating one measure of the electrical power of a signal. Thus, for an electrical engineer, power and variance of voltage are intimately related.

As with the term *signal*, the engineering term *power* has been co-opted by the purveyors of spectral analysis. Just as we can talk about the signal of a temporal series of wave heights, we can talk about the series' power, power being an informal substitute for the more appropriate term—variance. Similarly, when exploring the spatial variation in beetle density, the power of the signal has nothing to do with how much energy the insects expend; it is simply the variance of their density.

Note also that the term *power* as used in spectral analysis is different from power as used in inferential statistics. The power of a statistical test refers to its ability to distinguish accurately between the sample means of two populations.

2 FOURIER SERIES

With this terminology in hand, we can proceed to spectral analysis itself. Our first objective is to find a means of describing signals mathematically. Once we have a mathematical model of a given signal, we are then in a position to analyze its pattern. To begin, let's pick back up with our example of ocean waves.

Consider the simple water wave shown in Figure 20.2A. Measured at one point in space, water's surface varies sinusoidally through time, fluctuating up and down around average sea level, $\overline{z}$. For this simple signal,

$$z(t) = \overline{z} + \eta_{\max}\cos(2\pi f t). \tag{20.7}$$

Here $\eta_{\max}$ is the wave's *amplitude* (m), the magnitude of its maximum deviations, and f is the wave's *frequency* (cycles per second, Hz), the number of wave peaks that move past us in unit time. The product $2\pi f t$ is the wave's *phase*, measured in radians. Because the cosine is periodic, the signal starts over again every time $f t$ is an integer. Relative to mean sea level, *elevation* η is

$$\begin{aligned}\eta(t) &= z(t) - \overline{z} \\ &= \eta_{\max}\cos(2\pi f t).\end{aligned} \tag{20.8}$$

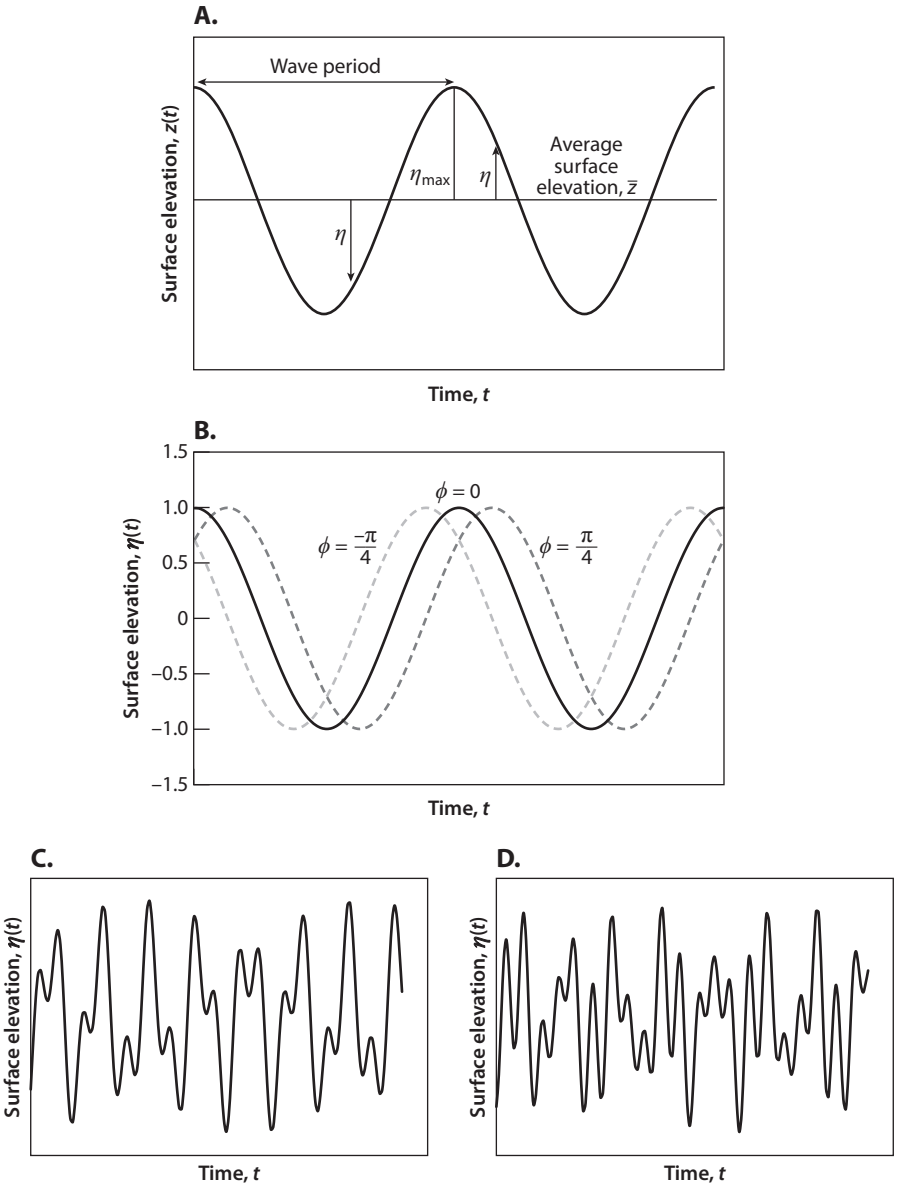

Figure 20.2 **A**. Nomenclature of an ocean wave. **B**. The phase shift, ϕ, adjusts the position of the wave in time or space. **C**. The sum of two waves yields a more complex waveform. **D**. The sum of three waves can be even more complex.

This model of the elevation signal assumes that the start of our measurements coincides with the arrival of a peak, that is, that at $t = 0$, $\eta(t) = \eta_{\max}$. If that isn't the case, we need to adjust equation 20.8 to account for the difference in time between the initiation of measurements and the arrival of a peak. This is achieved by including a term for the *phase shift*, ϕ, the angle (in radians) corresponding to the temporal shift in the signal:

$$\eta(t) = \eta_{\max} \cos(2\pi f t - \phi). \tag{20.9}$$

Now the first peak ($\eta_{\max}$) occurs at our site when $t = \phi/(2\pi f)$. By varying ϕ between $-\pi$ and π, we can adjust our model to match the temporal location of any wave (Figure 20.2B).

So far, I have described the wave as it varies through time at a particular location. We could describe the wave equally well as a function of location at a particular time. In this case,

$$\eta(x) = \eta_{\max} \cos(2\pi f_s x - \phi), \tag{20.10}$$

where x is distance measured along the path of wave propagation and f_s is *spatial frequency*, the spatial analog of temporal frequency:

$$f_s = \frac{1}{\lambda}. \tag{20.11}$$

Here λ is wavelength, the distance between successive wave crests.

For simplicity, I will introduce spectral analysis primarily as it relates to a temporal series, but the same principles apply to data measured in space. To model a spatial signal, one simply substitutes x for t and f_s for f; everything else is the same.

To this point, we have conjured up the mathematical description of a single sinusoidal wave, a far cry from the complex signals encountered in nature (e.g., Figure 20.1B, C). Let's see what happens if we combine two of these simple waves with different frequencies and (if we desire) different amplitudes and phases. When combining waves, we assume that they are strictly additive (i.e., each is unaffected by the presence of the other), an assumption known as the *principle of superposition*. In this case,

$$\eta(t) = \eta_{\max,1} \cos(2\pi f_1 t - \phi_1) + \eta_{\max,2} \cos(2\pi f_2 t - \phi_2). \tag{20.12}$$

This simple sum can take on a surprising variety of forms (e.g., Figure 20.2C). Adding a third sinusoid,

$$\eta(t) = \eta_{\max,1} \cos(2\pi f_1 t - \phi_1) + \eta_{\max,2} \cos(2\pi f_2 t - \phi_2) + \eta_{\max,3} \cos(2\pi f_3 t - \phi_3). \tag{20.13}$$

allows us to simulate even more complexity (e.g., Figure 20.2D).

Taken to its logical limit, this concept suggests that with a sufficient number of waveforms, each with an appropriate amplitude and phase, any given pattern of ocean waves can be accurately modeled. Expressed mathematically, we can suppose that

$$\eta(t) = \sum_{i=1}^{\infty} \eta_{\max,i} \cos(2\pi f_i t - \phi_i), \tag{20.14}$$

a suggestion that is, in fact, correct.

The same logic applies not only to ocean waves, but to any signal in nature. In other words, for an arbitrary signal $y(t)$,

$$y(t) = \overline{y} + \sum_{i=1}^{\infty} y_{\max,i} \cos(2\pi f_i t - \phi_i). \tag{20.15}$$

Or, for the signal expressed relative to its mean,

$$y(t) = \sum_{i=1}^{\infty} y_{\max,i} \cos(2\pi f_i t - \phi_i). \tag{20.16}$$

For simplicity, in the rest of this chapter we will assume that signals are measured relative to their means, allowing us to dispense with $\overline{y}$.

Equation 20.16 is simple, important, and (I hope) intuitive, but it leaves open two important questions. First, how does one choose the specific frequencies (f_i) to best model a particular signal? And then, how does one choose the amplitudes ($y_{\max,i}$) and phase shifts (ϕ_i) that correspond to those frequencies? We answer these questions in turn.

3 CHOOSING FREQUENCIES

The Role of Harmonics

The standard method for choosing component frequencies was formulated in the early 1800s by the same Jean Baptiste Joseph Fourier we encountered when exploring the conduction of heat in Chapter 12. The method begins by defining a series' *fundamental frequency*.

Just as for each string on a guitar there is a lowest note that it can play, there is for each time series a lowest frequency of fluctuation the series can accurately model. Consider, for instance, air temperature, which flucutuates both daily with the solar cycle as well as with the longer periods of the weather and seasons. If we measure temperature every minute for 24 h, our record will contain one full daily cycle, allowing us to describe the dial rhythm in detail. But having measured temperature for only a day, we don't have enough information to accurately describe weather-driven and seasonal fluctuations. In other words, just as the length of a guitar string determines its lowest note, the length of our record (in this case, 24 h) sets the lowest frequency of temperature fluctuation—the *fundamental frequency*—that we can reliably model.

We can generalize this conclusion. If we measure a signal for a total period $t_{\max}$, the lowest frequency we can model—the fundamental frequency—is

$$f_f = \frac{1}{t_{\max}}. \tag{20.17}$$

It is important to note that the fundamental frequency is set not by the signal itself, but rather by the way in which we measure it: the longer our record, the lower the fundamental frequency.

Now to the task of choosing the frequency of the sinusoids to use when modeling a particular signal. In a stroke of genius, Fourier proposed that a signal can be modeled most expeditiously using only those frequencies that are integral multiples of the fundamental. That is,

$$y(t) = \sum_{k=1}^{\infty} y_{\max,k} \cos\left(2\pi k f_f t - \phi_k\right). \tag{20.18}$$

Here k ($= 1, 2, \ldots, n$) designates the *harmonic* of each component sinusoid. For example, f_f is its own first harmonic, $2f_f$ is the second harmonic of the fundamental, and so forth. In practice, it is never possible to extend this series to an infinite number of harmonics (a topic we will deal with shortly), but the higher the harmonic included, the finer the detail that can be modeled.

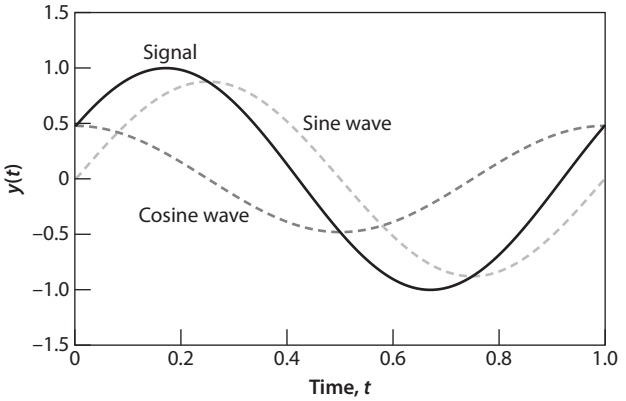

Figure 20.3 The sum of a sine wave and a cosine wave (the signal) is a sinusoidal wave, shifted in phase, with an amplitude that is a function of the amplitudes of the contributing waves.

Equation 20.18 is one form of the *Fourier series*, and it forms the basis of spectral analysis. As noted previously, one can easily adjust the Fourier series to describe a spatial rather than a temporal signal: just substitute x for t and spatial frequency (f_s) for temporal frequency (f).

To summarize: once we have measured a signal (thereby setting $t_{\max}$ and f_f), the choice of radian frequencies to use in modeling $y(t)$ is fixed—we use only harmonics of the fundamental frequency: f_f, $2f_f$, $3f_f$, and so on.

4 FOURIER COEFFICIENTS

Although equation 20.18. is a useful model, there are advantages to modifying its form. The basic idea behind this modification is that each component sinusoid in the Fourier series (with a certain amplitude and phase) can itself be modeled as the sum of a cosine wave and a sine wave, both having the same frequency as the component they model. For example, the sinusoid in Figure 20.3 (with $f = 1$, $y_{\max} = 1$, and $\phi = 0.5$) can be precisely modeled as the sum of a cosine wave (with $f = 1$ and an amplitude α of 0.878) and a sine wave (again with $f = 1$, but with an amplitude β of 0.479). In general terms, it can be shown (Supplement 20.1) that

$$y_{\max,k} \cos\left(2\pi k f_f t - \phi_k\right) = \alpha_k \cos\left(2\pi k f_f t\right) + \beta_k \sin\left(2\pi k f_f t\right), \tag{20.19}$$

where

$$y_{\max,k} = \sqrt{\alpha_k^2 + \beta_k^2} \tag{20.20}$$

and

$$\phi_k = \arctan\left(\frac{\beta_k}{\alpha_k}\right). \tag{20.21}$$

The larger α_k and β_k are, the greater the amplitude of the signal is; the larger β_k is relative to α_k, the greater the phase shift is.[1]

Because the sum of a cosine and a sine wave can mimic the effects of $y_{\max}$ and ϕ_k, we can rewrite the Fourier series (equation 20.18) as:

$$y(t) = \sum_{k=1}^{\infty} \left[\alpha_k \cos\left(2\pi k f_f t\right) + \beta_k \sin\left(2\pi k f_f t\right)\right]. \tag{20.22}$$

This is the form of the Fourier series used in spectral analysis. The α and β values in this series—the amplitiudes of the component cosine and sine waves, respectively—are known as *Fourier coefficients*. Again, one can easily adjust this series to describe a spatial rather than a temporal signal; just substitute x for t and fundamental spatial frequency ($f_{s,f}$) for fundamental temporal frequency (f_f).

To recap, by choosing the appropriate values for α and β in equation 20.22, and, by using a sufficiently high number of harmonics (k), we can model any signal we desire.[2]

5 THE PERIODOGRAM

Let's postpone for the moment the obvious question of how one would choose appropriate αs and βs. Instead, let's suppose that by some means we have obtained the full set of Fourier coefficients for a signal of interest, providing us with an accurate mathematical model of our signal. We can now use that information to answer our original question—how is the overall variance of a signal divided up among frequencies?

To begin, let's calculate the variance of a generic cosine wave,

$$y(t) = \alpha \cos(\theta). \tag{20.23}$$

Here, as with our ocean waves, $y(t)$ is the deviation from average, α is the cosine's amplitude, and for simplicity I have replaced $2\pi f t$ with θ. Thus, if we sample the waveform at n equally spaced points in one of its cycles, we can calculate its variance—its mean squared deviation. Recalling that the mean of a cosinusoidal oscillation is zero,

$$\begin{aligned}\sigma_y^2 &= \frac{1}{n}\sum_{i=1}^{n}\left[\alpha^2 \cos^2(\theta_i) - 0\right] \\ &= \frac{\alpha^2}{n}\sum_{i=1}^{n}\cos^2(\theta_i).\end{aligned} \tag{20.24}$$

[1] In case you've forgotten your trigonomtery, arctan(x) (the arctangent of x) is the angle whose tangent is x.

[2] There are some discontinuous mathematical functions that cannot be modeled by the Fourier series, but these functions seldom if ever appear in nature.

Now, if we have n points spread evenly across θ from 0 to 2π , the increment between two points is

$$\Delta\theta = \frac{2\pi}{n}. \tag{20.25}$$

Multiplying equation 20.24 by one in the form of $\Delta\theta/\Delta\theta$,

$$\begin{aligned}\sigma_y^2 &= \frac{\alpha^2}{n}\frac{1}{\Delta\theta}\sum_{i=1}^{n}\cos^2(\theta_i)\,\Delta\theta \\ &= \frac{\alpha^2}{2\pi}\sum_{i=1}^{n}\cos^2(\theta_i)\,\Delta\theta.\end{aligned} \tag{20.26}$$

Allowing $\Delta\theta$ to become small, we can take this relationship to its integral form:

$$\sigma_y^2 = \frac{\alpha^2}{2\pi}\int_0^{2\pi}\cos^2(\theta)\,d\theta. \tag{20.27}$$

Unless you are adept at calculus, you would have some difficulty evaluating the integral in this equation, but it is easy to look up the solution:

$$\int_0^{2\pi}\cos^2(\theta)\,d\theta = \pi. \tag{20.28}$$

Thus,

$$\sigma_y^2 = \frac{1}{2}\alpha^2. \tag{20.29}$$

In other words, the variance of a cosine wave is equal to half the square of the wave's amplitude.

The same logic can be applied to a sine wave [$y(t) = \beta\sin(\theta)$]—variance is again half the square of amplitude:

$$\sigma_y^2 = \frac{1}{2}\beta^2 \tag{20.30}$$

We can extend this logic even further. Because the sum of cosine and sine waves is a sinusoid with amplitude $\sqrt{\alpha^2+\beta^2}$ (equation 20.20) the variance of each combination of harmonic cosine and sine waves in the Fourier series is

$$\sigma_{y,k}^2 = \frac{1}{2}\left(\alpha_k^2+\beta_k^2\right). \tag{20.31}$$

Let's pause for a moment to take stock of where we have come. The task we assigned ourselves in this chapter was to characterize the pattern of a signal by determining how its overall variance is divided up among component frequencies. Perhaps without your realizing it, equation 20.31 is the answer. If we know the Fourier coefficients for a signal—the αs and βs—equation 20.31 tells us how to calculate the variance for each harmonic component and, therefore, how to specify the variance at each harmonic frequency.

This is the heart and soul of spectral analysis. As such, it deserves a means of visualization. A graph of the harmonic component variances (σ_k^2) as a function of frequency is called a *periodogram*. Figure 20.4A shows hypothetical (but realistic) results for ocean waves. It is clear that the overall variance in elevation cannot be attributed to any single frequency; instead it is distributed among frequencies. In this

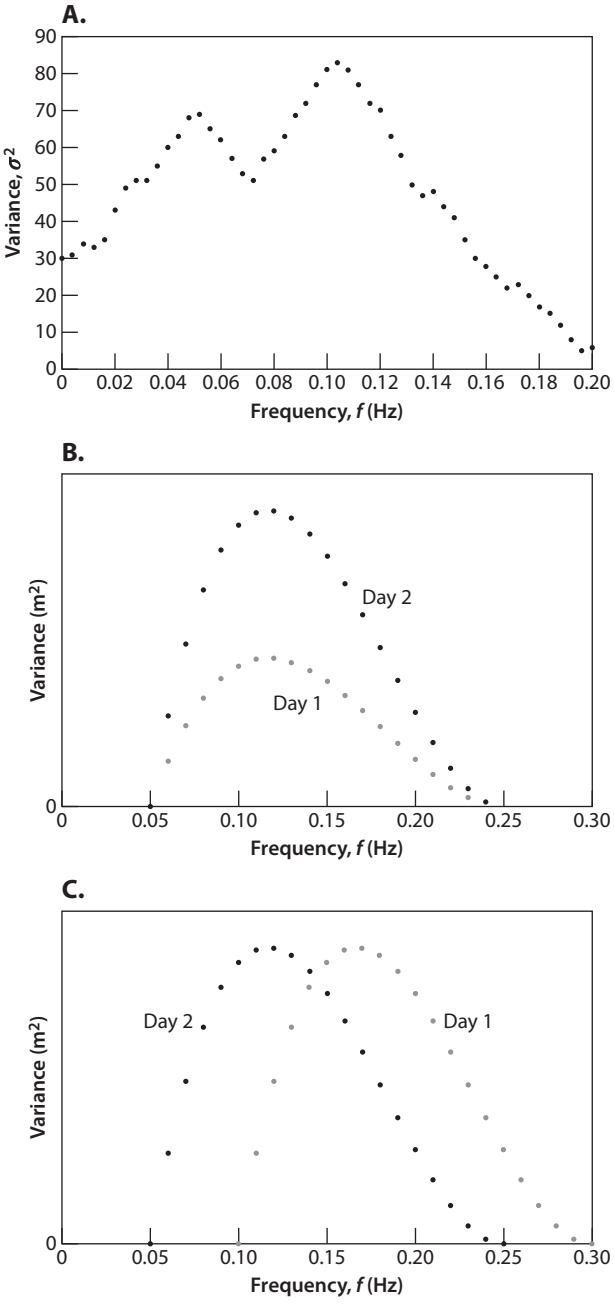

Figure 20.4 **A**. The periodogram for a hypothetical sea state. Hypothetical periodograms for two sea states: **B**. the same frequency distribution, different variances; **C**. the same variance, different frequency distributions.

case, much of the overall variance is associated with frequencies corresponding to individual waves ($f \approx 0.1$ Hz) and much of the remainder with frequencies typical of groups of waves (a phenomenon known as surf beat, $f \approx 0.05$ Hz).

One last step and we can bring this discussion full circle. Because the harmonic components of a signal act independently of each other (a result of the superposition principle), the overall variance of the entire signal is the sum of its component variances:

$$\sigma_{\text{tot}}^2 = \frac{1}{2}\sum_{k=1}^{\infty}\left(\alpha_k^2 + \beta_k^2\right). \tag{20.32}$$

We started this chapter by noting that total variance is a blunt instrument for characterizing pattern. We have now returned to the total variance, but equation 20.32 makes it explicit how the various harmonic components contribute.

To get a feel for the utility of the periodogram, consider the scenario depicted in Figure 20.4B, the periodograms for ocean waves measured on two different days. In this case, waves on the two days have the same frequency characteristics (swell with frequencies centered on 0.12 Hz), but day 2 is wavier than day 1—that is, the overall variance (the sum of individual variances) is greater.

The periodograms shown in Figure 20.4C tell a different story. The sum of values in each of the two periodograms is the same, so we can deduce that the waviness of the ocean (the total variance) was the same on both days. However, on day 1, wave frequencies were centered around 0.18 Hz, whereas on day 2, frequencies were centered around 0.12 Hz. In other words, the days were equally wavy (they had the same vaiance of surface elevation), but on day 1 waves were relatively high-frequency wind chop, while on day 2 they were relatively low-frequency swell.

6 SPECIFYING FOURIER COEFFICIENTS

As we have just seen, if all of a signal's Fourier coefficients are known, we can construct the periodogram. But, given a time series of measurements, how does one choose appropriate coeffcients? To answer this question, consider a short time series in which we have measured some signal y over n (= 4) intervals (Figure 20.5A). The constant interval between measurements is Δt, the *grain* of our measurements. The overall length of our series—its *extent*—is thus $n\Delta t$. What harmonics are required to best model this simple time series, and what values of α and β do they have?

Let's begin with f_f. As we have seen, the overall length of this series ($n\Delta t$) defines its fundamental frequency. Thus, according to equation 20.17;

$$f_f = \frac{1}{n\Delta t}. \tag{20.33}$$

In compliance with Fourier's insight, we therefore model the signal using harmonics of this fundamental frequency.

(Note for future reference that because the Fourier series deals with harmonics of the fundamental, the difference in frequency between successive harmonics (Δf) is the same as f_f itself. For example, the difference in frequency between the second and third harmonics (that is, Δf) is $3f_f - 2f_f = f_f$. This leads to an interesting conclusion: because $f_f = 1/t_{\text{max}}$, the longer the series of data, the smaller f_f is. The smaller f_f is, the smaller the difference in frequency between harmonics (Δf), and the greater the resolution with which we can analyze the frequency dependence of the overall variance. Long data series permit fine frequency resolution.)

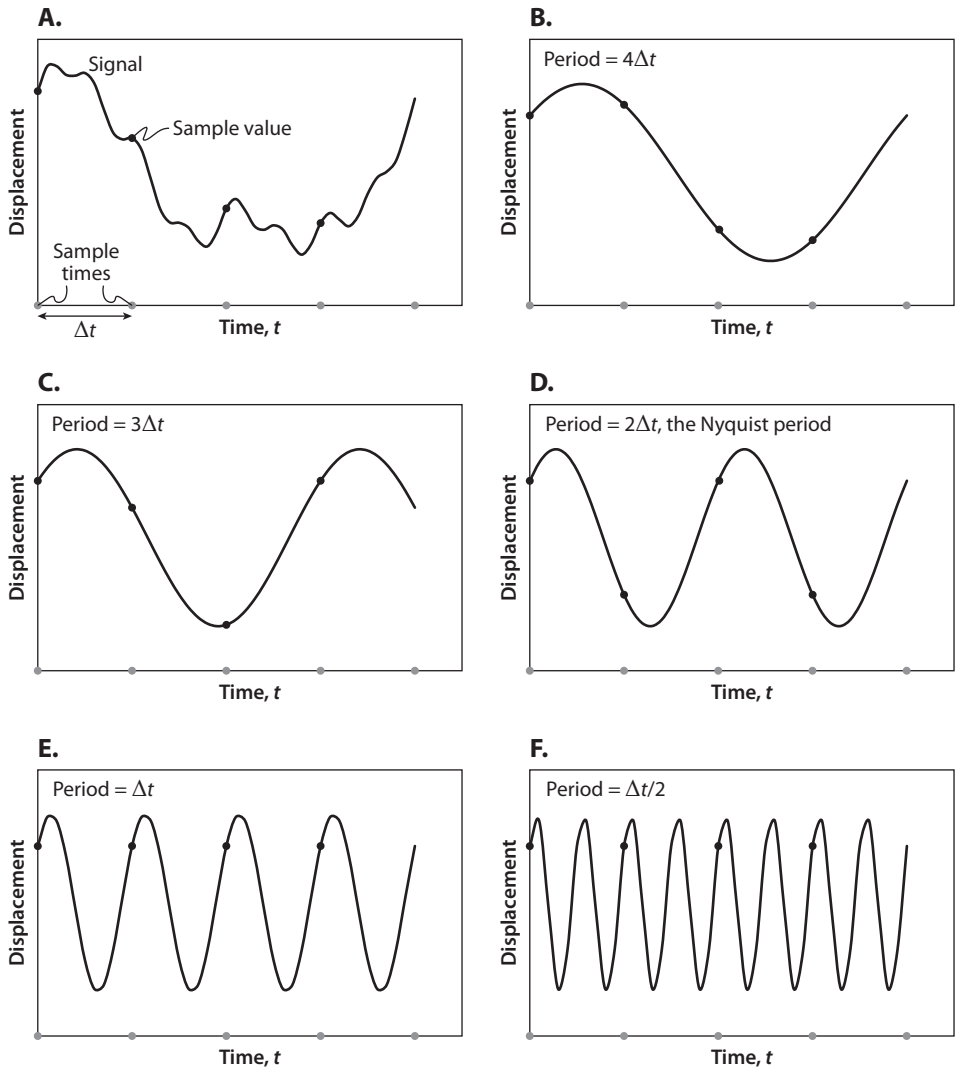

Figure 20.5 Determining the Nyquist period. We sample a signal at intervals of Δt to create a data series with four points (**A**). The ability to discern the components of the signal depends on each component's period. Our sampling regime captures the variation in signals with periods of $4\Delta t$ (**B**), $3\Delta t$ (**C**), and $2\Delta t$ (**D**) but not Δt (**E**) or $\Delta t/2$ (**F**).

Having established a series' fundamental frequency, you might suppose that we could then examine as many harmonics as we like; the more we use, the better we can describe the signal's high-frequency detail. There is a practical limit, however. Let's see what our sampling protocol tells us as we sample signals that represent increasing harmonics of the fundamental frequency. In Figure 20.5B, the signal oscillates with a period of $4\Delta t$; that is, its period of oscillation is equal to the fundamental period set by the length of our short data series. The measurements adequately sample the signal's fluctuations. (Note that if we were to include a fifth point in our sample at a time Δt farther along, it would coincide with the beginning of the second cycle of

oscillation and thus would be a redundant measure of the oscillation's behavior. The four points shown are sufficient.) Figure 20.5C shows a new signal with a period of $3\Delta t$ and, thus, a frequency higher than the series' fundamental frequency. Again, our measurements (spaced Δt apart) capture the signal's fluctuation. The same is true for a signal with period $2\Delta t$ (Figure 20.5D). By contrast, when presented with a signal that oscillates with a period of Δt, our measurements sample the signal only once in each period (Figure 20.5E). As a consequence, every measurement yields the same value, and, as far as our measurements can discern, there is no variance at that frequency. The same holds true for signals with periods less than Δt (e.g., Figure 20.5F). In short, we can detect harmonics with periods of $2\Delta t$ or greater but not harmonics with periods of Δt or less. Thus, the highest frequency we can detect (known as the *Nyquist frequency* or *Nyquist limit*[3]) corresponds to the shortest period we can effectively sample, $2\Delta t$:

$$f_{k_{\max}} = \frac{1}{2\Delta t}. \tag{20.34}$$

Recalling that the fundamental frequency is $1/n\Delta t$, we can calculate the harmonic ($k_{\max}$) corresponding to the Nyquist frequency:

$$\begin{aligned} f_{k_{\max}} &= \frac{1}{2\Delta t} = k_{\max}\frac{1}{n\Delta t} \\ k_{\max} &= \frac{n}{2}. \end{aligned} \tag{20.35}$$

In other words, if we there are n intervals in our time series, only the first $n/2$ harmonics in the Fourier series provide any information about the signal. Thus, the best we can do to approximate the actual signal is the series:

$$y(t) = \sum_{k=1}^{n/2} \left[\alpha_k \cos\left(2\pi k f_f t\right) + \beta_k \sin\left(2\pi k f_f t\right)\right]. \tag{20.36}$$

This is both good news and bad news. The bad news is that because measured time series always have finite length, our ability to analyze the details of their high-frequency fluctuations is limited to frequencies at or below the Nyquist limit. The good news is that we have to estimate αs and βs for only a limited number of harmonics.

Now to that nagging practical question: how do we find the $n/2$ values for α and β that allow equation 20.36 to best approximate $y(t)$? The algorithms involved are a bit intense, and I refer you to Supplement 20.2 for the details, but an example can convey the calculations' essence—αs and βs are calculated through a series of linear regressions.

Consider a series of 120 daily measurements of water level in an alpine lake (Figure 20.6A). It's clear that water level fluctuates more or less periodically, and our job is to calculate the αs and βs that best describe this behavior. For each harmonic k of the fundamental frequency, we calculate α_k by correlating our water-level data with a cosine wave of amplitude 1 (a unit cosine) at the harmonic frequency. The slope of the regression line is our best estimate of α_k.

[3] Named for Harry Nyquist (1889–1976), an electrical engineer working at Bell Laboratories.

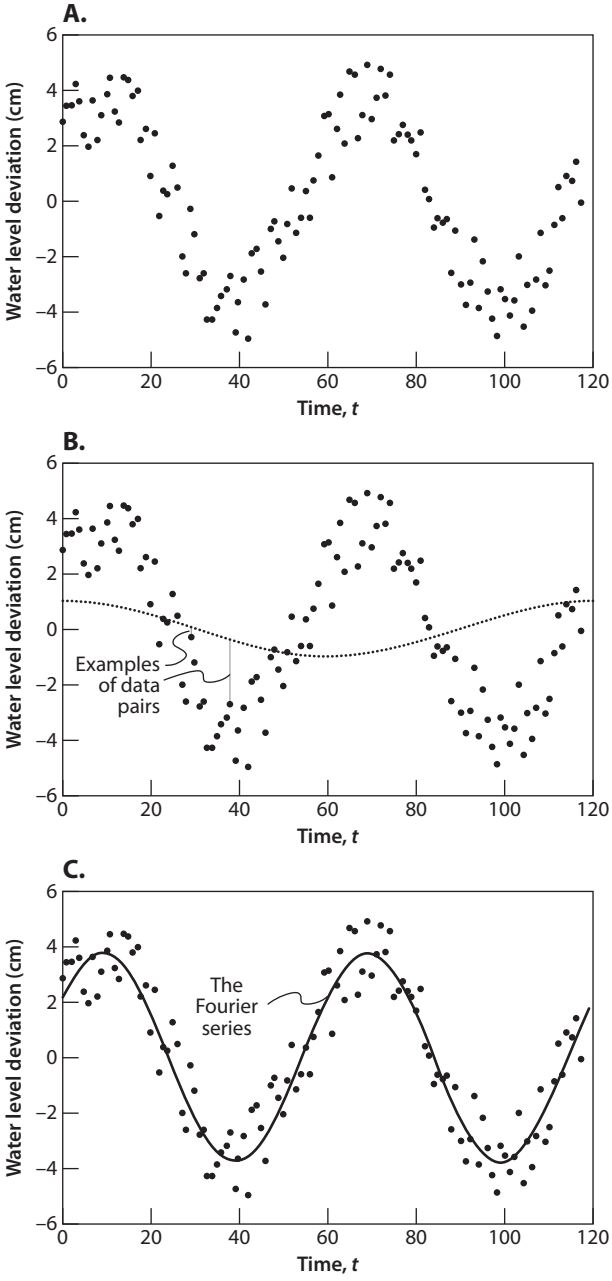

Figure 20.6 Quantifying Fourier coefficients. **A**. The measured record of water level. **B**. Points in the measured record are paired with points of a unit cosine wave of the fundamental frequency. **C**. The calculated fit to the empirical data.

For example, in Figure 20.6B, the measured data are shown along with a unit cosine at the series' fundamental frequency. The water level at time t_1 can be matched with the value of the cosine at time t_1, the level at t_2 with the cosine at t_2, and so on. A plot of all these pairs (one versus the other) is shown in Figure 20.7A. There is a pattern to

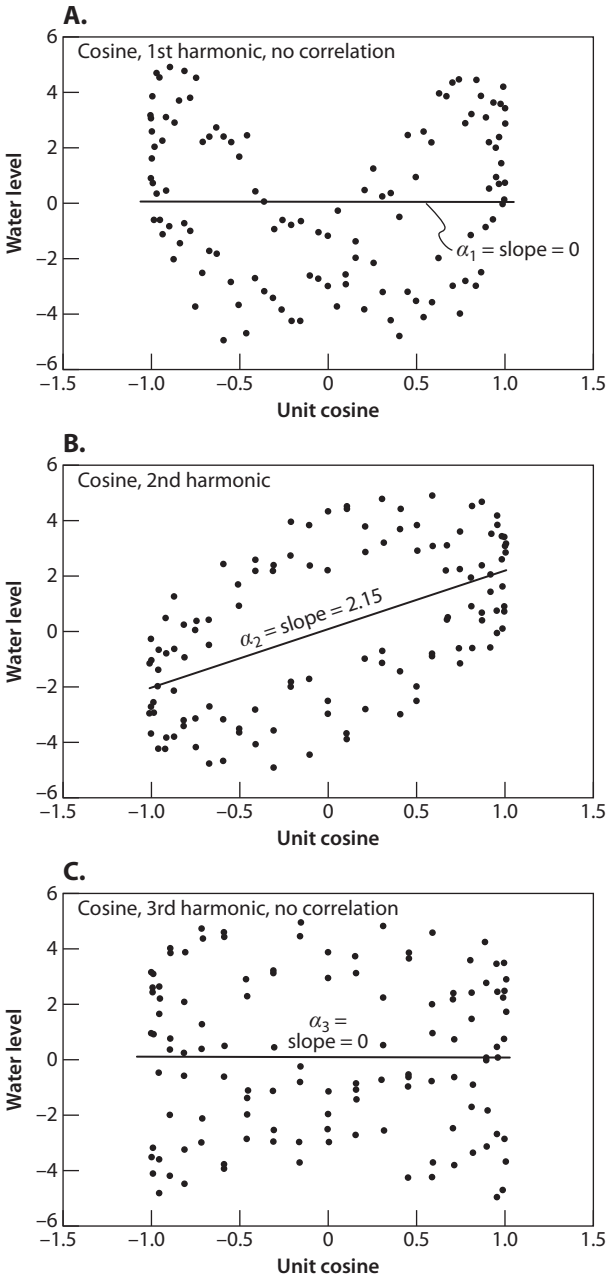

Figure 20.7 Calculating Fourier coefficients: α (**A**–**C**) and β (**D**–**F**) for the first three harmonics of the water-level signal from Figure 20.6.

this plot but no correlation between the measured data and the cosine—when we fit a line to the graph (a linear regression), we find that it's slope is zero. This tells us that $\alpha_1 = 0$.

I have repeated this procedure for unit cosine waves at the second and third harmonics of the fundamental, with the results shown in Figure 20.7B and C,

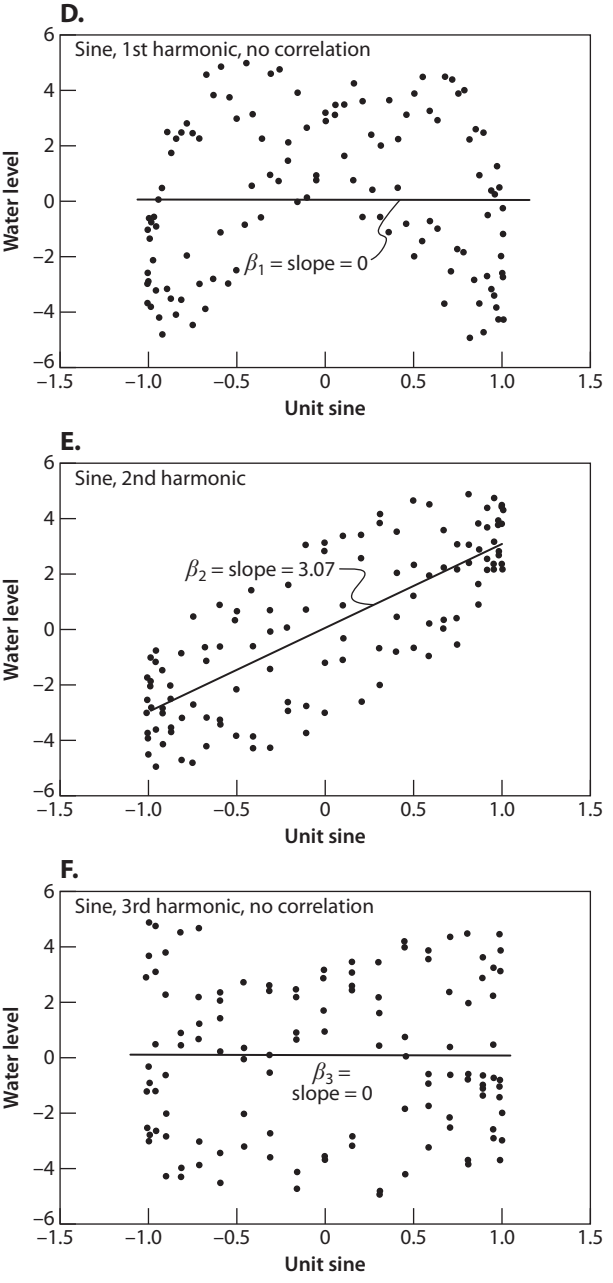

Figure 20.7 Continued.

respectively. For the second harmonic, there is a substantial correlation, and the regression line has a slope of 2.15, so $\alpha_2 = 2.15$. For the third harmonic, there is no correlation and $\alpha_3 = 0$. This procedure could be repeated for higher harmonics to calculate α_4 to $\alpha_{k_{\max}}$.

This whole process can then be repeated using unit sine (rather than cosine) waves (Figure 20.7D–F) to calcutate β_1 to β_3. The first and third sine harmonics show no

correlation and their regression lines have zero slopes, so β_1 and β_3 are zero. But the data are correlated with the second sine harmonic, and the slope of the regression line is 3.07, so $\beta_2 = 3.07$.

Using the these calculated αs and βs, we can calculate the sum of an abbreviated Fourier series, with results shown in Figure 20.6C. Lo and behold, this sum nicely models the major trend in the measured data, an oscillation at a frequency twice the fundamental of the data series. If we were to extend our efforts to higher harmonics, we would obtain an ever better model of our measurements.

This example is intended to give you insight into the process by which α and β are estimated. It is unlikely, however, to give you a feel for the large number of calculations involved. Estimating α and β is not something one does on a calculator or even in a spreadsheet. Indeed, until 1965 when J. E. Cooley and J. W. Tukey invented the Fast Fourier Transform (FFT), calculating αs and βs for a long series was taxing even for computers. The FFT drastically increases the computational efficiency of calculating αs and βs, and algorithms for the FFT are now included in most programming languages.

In summary, given a series of data, methods are available to estimate α and β for all harmonic components from the fundamental to the Nyquist. With these parameters in hand, one can accurately model the signal, plot the periodogram, and proceed with its interpretation.

7 THE POWER SPECTRUM

There's just one hitch. Although the periodogram admirably portrays how overall variance is divided among frequencies, this is not how the results are traditionally presented. Instead, the frequency-dependent characteristics of a signal are most often graphed as a *power spectrum*, where, as noted earlier, the term power is a stand-in for variance. To understand the switch—and the reason for undertaking it—we begin with a brief digression to statistics.

You may recall from an introductory stats class that the probability of seeing a particular outcome in an experiment can often be calculated using the binomial distribution. A classic example is an experiment in which you toss a coin 10 times and ask what the probability is that you will get a certain number of heads. The answer is provided by the binomial distribution (Figure 20.8A) in which each number of heads—from 0 to 10—is associated with a specific probability. There is, for instance, an 11.72% chance of getting 7 heads in 10 tries (see Denny and Gaines (2000) for an explanation of the binomial distribution).

But calculating binomial probabilities for a large number of trials is laborious. As a practical alternative, statisticians instead rely on the fact that, when dealing with many trials, the binomial distribution approximates a normal (Gaussian) distribution (Figure 20.8B), which is much more easily calculated. In fact, for an infinite number of trials, the two distributions are functionally equivalent, with one important difference. Whereas the binomial distribution specifies a probability for each outcome, the normal distribution provides a *probability density*, the probability per *range* of outcomes. The reason is this: in an infinite number of trials, there is an infinite number of ways that an experiment can play out, so the probability of getting any particular number of heads is effectively zero. A graph of this distribution (an infinite series of zeros) would therefore look like a bare set of axes, a totally uninformative picture.

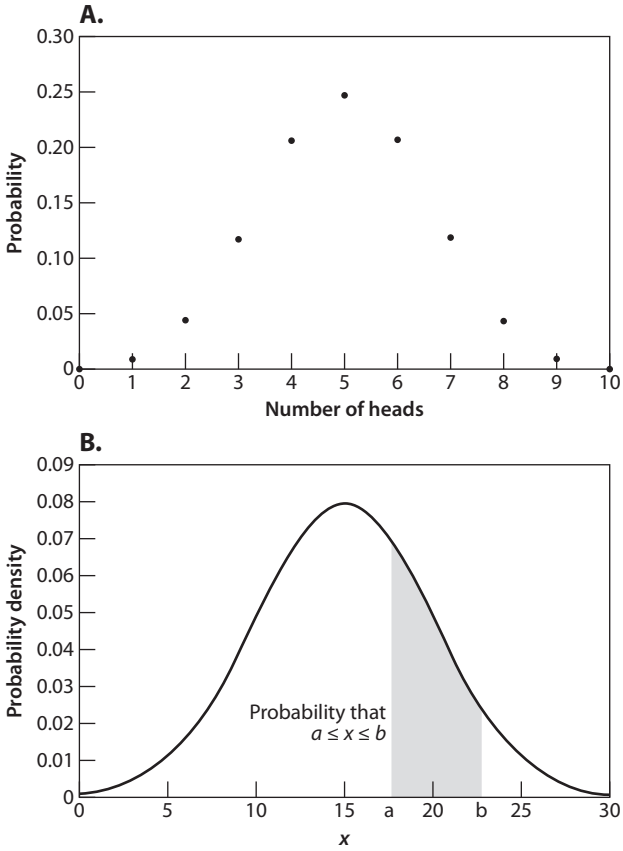

Figure 20.8 Representative binomial (**A**) and normal (**B**) distributions.

When dealing with an infinite number of trials, the best we can do is describe not the probability of each individual outcome, but rather the probability that an outcome chosen at random will fall within a certain range of values.

The normal distribution provides this description. To extract a probability value from a normal curve, one calculates the area under the probability density function corresponding to a given range of outcome values (Figure 20.8B). Because the function covers the probability of all possible outcomes, the total area under the curve is 1.

The power spectrum results from an analogous thought process. From equation 20.31 we know that the variance at each individual harmonic k is

$$\sigma_k^2 = \frac{1}{2}\left(\alpha_k^2 + \beta_k^2\right). \tag{20.37}$$

Using the same logic as before, we can surmise that the variance associated with individual harmonics is likely to decrease as the number of harmonics in the Fourier series increases, and as we have seen, the number of harmonics we can examine $(n/2)$ increases with n, the number of intervals in our series. Thus, as we increase the number of measurements in an attempt to discern more detail in a signal, we simultaneously decrease the magnitude of the variance estimate for each individual

frequency.[4] Taken to its logical extreme, this suggests that if we were to measure a signal continuously—that is, at an infinite number of points—our ability to say anything about the distribution of variance would vanish.

To rescue the periodogram from this fate, we need to adjust our expression describing the variance at each harmonic. To counteract the decrease in σ_k^2 as n increases, we multiply σ_k^2 by a term that increases with n. For reasons that will become clear in a moment, we choose $n\Delta t$. Thus our new variable—the *power spectrum*, S—is the product of σ_k^2 and $n\Delta t$. Evaluating S for the kth harmonic,

$$S_k = n\Delta t\sigma_k^2 = \frac{n\Delta t}{2}\left(\alpha_k^2 + \beta_k^2\right). \tag{20.38}$$

We could plot these data as a function of frequency for a spectral equivalent of the periodogram.[5]

Having defined S in this manner, we can immediately turn the definition around. At each individual harmonic,

$$\sigma_k^2 = \frac{S_k}{n\Delta t}. \tag{20.40}$$

But we know from equation 20.33 that

$$\frac{1}{n\Delta t} = f_f. \tag{20.41}$$

Furthermore, as noted previously, because the Fourier series calculates variance at harmonics of the fundamental frequency, Δf, the difference in frequency between harmonics, is equal to f_f. Thus, at each harmonic,

$$\sigma_k^2 = S_k\Delta f, \tag{20.42}$$

and summed across harmonics,

$$\sigma_{\text{tot}}^2 = \sum_{k=1}^{n/2} S_k\Delta f. \tag{20.43}$$

To this point, we have simply come up with another way of stating equation 20.32, the equation that gave us the periodogram. The value of these machinations appears when n becomes very large. Taken to the limit as n approaches infinity, Δf becomes df, and

$$\sigma_{\text{tot}}^2 = \int_0^\infty S\,df. \tag{20.44}$$

In other words, the overall variance of a signal is equal to the area under the curve of its power spectrum. Furthermore, the variance associated with any range of frequencies

[4] Only if a harmonic *exactly* matched the perfectly constant frequency of a signal would amplitude stay constant as the number of harmonics increases. For real-world signals, an exact match and perfect constancy are essentially impossible.

[5] There is one exception to this rule. At the Nyquist frequency, $k = n/2$:

$$S_{k_{\max}} = n\Delta t\alpha_{k_{\max}}^2. \tag{20.39}$$

The difference of a factor of 2 in the form of this expression is due to the fact that $\beta_{k_{\max}} = 0$ (see Supplement 20.2).

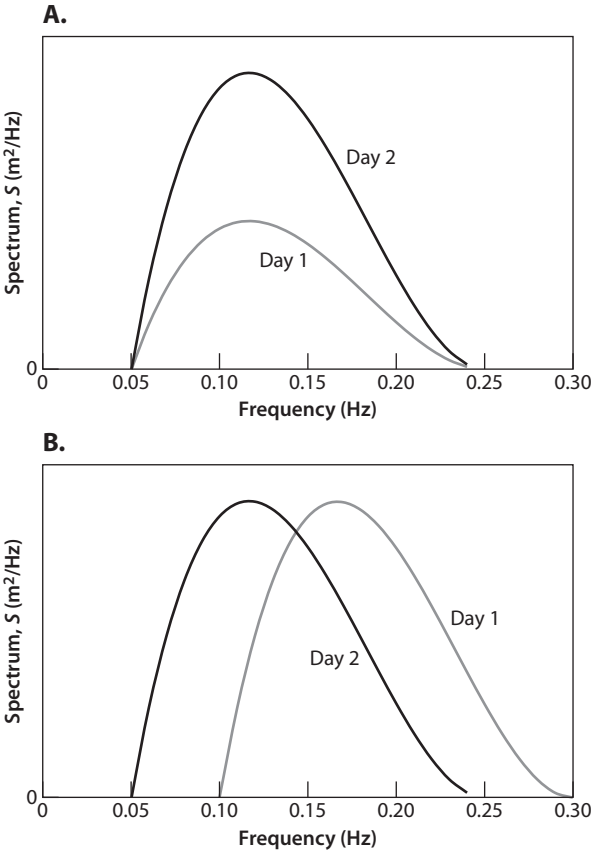

Figure 20.9 Hypothetical spectra for ocean waves. **A**. Two sea states with the same frequency distribution but different variances. **B**. Two sea states with the same variance but different frequency distributions.

is the area under that portion of the overall spectrum. For example, the variance in the range between $f = a$ and $f = b$, is

$$\sigma^2_{a,b} = \int_a^b S\, df. \tag{20.45}$$

Let's consider some hypothetical spectra for ocean waves (Figure 20.9). In panel A, surface elevations recorded on two days have the same frequency characteristics, but day 2 is wavier than day 1 (the variance in surface elevation is greater) because the area under its spectrum is greater. We draw different conclusions from the spectra shown in Figure 20.9B. In this case, because the area under the two spectra is the same, we can deduce that the waviness of the ocean was the same on both days. However, on day 1, wave frequencies were centered around 0.18 s^{-1}, whereas on day 2, wave frequencies were centered around 0.12 s^{-1}. In other words, the days were equally wavy, but on day 1 the waves were wind chop, while on day 2 they were swell.

These examples should give you an intuitive feel for how to interpret the spectra you might encounter in the literature. But at this point, you might be scratching your head. The spectra in Figure 20.9 correspond exactly to the periodograms in Figure 20.4.

Since the spectrum doesn't contain any more information than the periodogram, why bother with the translation?

The answer is twofold. Recall from the preceding discussion that construction of a spectrum assumes that the signal can be described continuously. This is impossible for real-world measurements (one would need an infinite series of data) but is easy in a theoretical model. For instance, a mathematically inclined physical oceanographer might assume a particular size and shape for the power spectrum of ocean waves. He or she could then express the spectrum as a continuous function of f, and proceed to evaluate its properties according to equation 20.45.

By contrast, spectra calculated from real-world data are, at their core, always periodograms. Because actual measurements can be made only at discrete times and for a finite period, the Fourier series can be calculated for only a finite number of frequencies. In this respect, it would be best if the data were presented as a periodogram rather than translating them into a spectrum with its implied aura of continuity. But that sort of truth in advertising would raise another problem. Consider a study in which theory and measurement are combined, the goal being to use theory to predict the real world. If the theoretical results were presented as a spectrum and the measured results as a periodogram, it would be difficult for the reader to compare them quantitatively. The traditional solution to this problem is to present data (both theoretical and measured) as spectra. As long as you keep in mind that any spectrum resulting from measured data is really a series of individual points, no problems should arise.

8 SPECTRAL ANALYSIS IN BIOLOGY

8.1 Population Cycles in Snowshoe Hares

We will put spectral analysis to use in Chapter 21 when we consider the issue of scaling in ecology, but to provide a preview of the grandeur to come, let's explore two examples of the utility of spectral analysis in ecomechanics.

Populations of arctic mammals often cycle through periods of boom and bust (Krebs et al. 2001), the classic case being the decadal cycle of snowshoe hares. Several factors contribute to the periodic fluctuations in hare populations—the availability of food, predation by lynx and birds, and the physiological response of hares to the stress in their lives—but, remarkably, despite the inherently local nature of these drivers, cycles of population fluctuation are synchronized across vast areas. Hare populations in much of the Canadian Arctic fluctuate in unison across habitats that differ drastically in precipitation, average temperature, terrain, and flora.

It has long been speculated that maintenance of this synchronicity requires cues from some external time giver, some factor—presumably one in the physical environment—that applies equally across all local populations. In an influential paper in 1993, Sinclair and colleagues made the brash suggestion that sunspots provided the necessary cue.

In support of this proposition, Sinclair and his colleagues obtained a lengthy time series of hare population density, relying on indirect evidence from tree rings. When populations are dense, hares are forced to eat the growing tips of spruce trees for

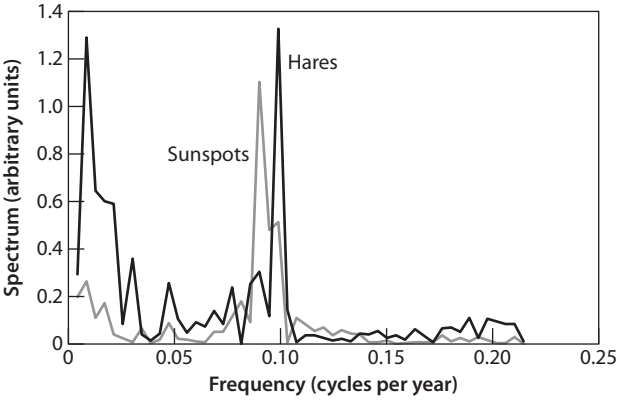

Figure 20.10 The spectra for snowshoe hares and sunspots (drawn from data in Sinclair et al. 1993).

winter forage.[6] A nipped tip leaves a dark mark in the subsequent tree ring, thereby providing a history of hare population cycles back to the eighteenth century.

The periodic fluctuation in sunspots has been recorded by astronomers for the same period, and when Sinclair and colleagues compared the power spectra of the two phenomena, they matched within the resolution of the technique; both have spectral peaks at frequencies (cycles per year) of 0.090 to 0.099 (Figure 20.10). With this suggestive evidence in hand, they proceeded to analyze their data in greater depth, concluding that during times of elevated solar activity, not only do the sunspot and hare cycles have the same period, but they tend to maintain a constant phase relationship. When solar activity is low, the phase of the hare cycle gradually shifts, only to be brought back into synchrony when the sun acts up again.

The intriguing thought that something as distant and subtle as sunspots might act as a synchonizing influence in population biology has sparked considerable interest and controversy. The evidence of Sinclair and colleagues strongly suggests a mechanistic connection between solar activity and hare populations. However, experiments have elegantly demonstrated that the proximal causes of population fluctuations are predation pressure (from lynx, for instance) and its effects on hare reproductive efficiency (Krebs et al. 2001). If the solar cycle cues the system, it seems that it must act indirectly through this predator-prey relationship. Other than some vague ideas about climatic effects, Sinclair and his colleagues have not been able to identify a plausible mechanism, so the question of a connection between solar activity and snowshoe hares remains open.

However, the current lack of a mechanistic tie between hares and sunspots should not cause us to lose sight of the main point here. As with ice ages and celestial mechanics, without spectral analysis we wouldn't know that there was a phenemenon that required investigation.

[6] You might wonder how hares get to the tops of trees to eat their growing tips. This is the arctic, with its low temperatures and short growing season. A 50-y-old spruce tree is only about a meter high, within the reach of an adult hare.

8.2 Sea Urchins and Algal Dominance

In the nearshore waters of Japan, benthic seaweeds have a characteristic zonation. From the intertidal zone to a depth of 2 to 3 m, rocky substrata are covered by a dense canopy of kelps and red algae. Deeper, this canopy abruptly disappears, giving way to barren areas in which crustose corallines are the only seaweeds. From a strictly mechanical perspective, this zonation is perplexing. Kelps and red algae (which are susceptible to damage from breaking waves) are found only in the shallows where wave-induced velocities are highest, while crustose corallines (which are virtually immune to wave-induced disturbance) dominate where velocities are benign.

The answer to this paradox involves the interaction of seaweeds with their primary herbivore, the sea urchin *Strongylocentrotus nudus*. Where flow is slow, these urchins are effective grazers, but when average velocity exceeds $0.4\ \mathrm{m \cdot s^{-1}}$, they retreat to their burrows. Kawamata (1998) suggested that water velocity thus serves as an indirect control on algal abundance. Urchins can't feed in the shallows where water velocities are high, allowing seaweeds to flourish, even though some are damaged. Deeper, urchins are free to graze, forming the barrens. To test this hypothesis, however, he needed to predict how velocity varied with depth at his study site. This is where spectral analysis comes in.

From basic wave theory (Denny 1988), we know that maximum water velocity at the substratum (where urchins live) is a function of wave amplitude $\eta_{\max}$, wave frequency f, and depth of the water column d:

$$u_{\max}(f,d) = \sqrt{\eta_{\max}^2 U(f,d)^2}. \tag{20.46}$$

Here the function U describes how velocity varies with depth, depending on wave frequency:

$$U(f,d) = \frac{1}{\sinh\left[\frac{4\pi^2 f^2 d}{g\tanh\sqrt{\frac{4\pi^2 f^2 d}{g}}}\right]}. \tag{20.47}$$

Values of U are shown as a function of frequency and depth in Figure 20.11.[7] Provided we know wave amplitude and frequency, equations 20.46 and 20.47 allow us to calculate the velocity imposed on an urchin living at a certain depth.

Our analysis would be straightforward if waves had a fixed amplitude and frequency, but as we have seen, the ocean surface isn't that simple. Let's suppose that we have recorded surface elevation at a site where urchins live (e.g., Figure 20.2B). How can we use this messy empirical information about surface elevation to predict average velocity as a function of depth?

Of course, spectral analysis is the answer. From the empirical data, we can calculate the periodogram. From the periodogram, we know what $\eta_{\max}^2$ is for each component

[7] The hyperbolic sine and tangent (sinh and tanh) are defined as

$$\sinh(x) = \frac{1}{2}\left(e^x - e^{-x}\right), \tag{20.48}$$

$$\cosh(x) = \frac{1}{2}\left(e^x + e^{-x}\right), \tag{20.49}$$

$$\tanh(x) = \frac{\sinh(x)}{\cosh(x)}. \tag{20.50}$$

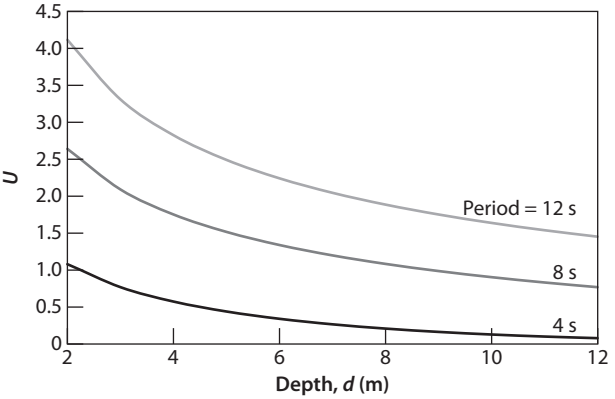

Figure 20.11 The function U used to calculate velocity as a function of wave period and water-column depth, d.

wave frequency f, and from these frequency-specific variances, we can use equations 20.46 and 20.47 to calculate each frequency's contribution to the overall velocity at a given depth. We then sum these frequency-specific velocities to calculate the overall average maximum velocity, $u_{\max}$. In short, in order to predict the velocities imposed on urchins as a function of depth, Kawamata needed to know not only the overall waviness at his site, but also how the variance of surface elevation was spread across frequencies.

To this end, he obtained periodograms for the surface elevation every day for five years. From these data, he followed a procedure similar to that described here to calculate daily average $u_{\max}$ as a function of depth, and from these he estimated the fraction of time available for urchins to feed. At 2 m depth, urchins could feed for less then 2.6% of the time, insufficient to keep seaweeds in check. At 10 m, they could feed more than 70% of the time, plenty of opportunity to maintain the algal barrens. Thus, with the help of spectral analysis, Kawamata could explain the distribution of his seaweeds.

9 CONCEPTS, CONCLUSIONS, AND CAVEATS

The mean and variance are insufficient to quantify the pattern of fluctuation in a sequence of data. At the very least, we need to take into account how overall variance is divided up among the component frequencies of the signal. This is a job for spectral analysis, which relies on the ability of the Fourier series to model a signal in time or space. By calculating α and β for the harmonic components of a signal, we can construct the data's periodogram and power spectrum, which allow us to make comparisons among signals (as Sinclair et al. did with the fluctuations in sunspots and arctic hares), to use the distribution of variance among frequencies to make other calculations (as Kawamata did to predict the effect of water velocity on urchin foraging), or to identify periodicities (as for the ice ages). We will put power spectra to use in the next chapter where we describe how the temporal or spatial scale at which an organism interacts with its environment affects the plant or animal's average response.

Be warned that this chapter has introduced spectral analysis only at a conceptual level. There are a whole host of details that need to be taken into account when the method is put to practical use. For example, spectral analysis as described here implicitly assumes that the process from which measurements are taken is *stationary*. Roughly speaking, a procees is stationary if the same statistics (e.g., the mean, variance, and spectrum) are obtained regardless of when or where the data series starts. Many ecological series violate this assumption—air temperature, for instance, is trending upward, so its mean changes through time—and these nonstationary series must be massaged into stationarity before they are analyzed. The brief discussion in Supplement 20.4 will introduce you to this and other issues in the practical use of spectral analysis, allowing you to bridge the gap to introductory texts such as Diggle (1990). Once you are comfortable with the basics, there are several excellent upper-level texts (e.g., Priestley 1981; Bendat and Piersol 1986).

Spectral analysis is only one of several methods available to explore the pattern of sequential data. *Wavelet analysis* is a notable alternative, with some distinct advantages. For example, spectral analysis considers a data series as a whole, correlating the data with cosine and sine waves that have the same extent as the entire data set (e.g., Figure 20.6B). As a result, spectral analysis can accurately quantify the contributions of various frequencies of oscillation to the over all variance, but it can't localize where within a series those oscillations occurred. When applied to the ice-age data in Figure 20.1A, for instance, spectral analysis can tell us that the variance in Earth's temperature has sustantial components at periods of 41,000 and 100,000 y, but it can't tell us that the 41,000-y oscillations ocurred at a diferent time than the 100,000-y oscillations. By contrast, wavelet analysis correlates data not with a continuous cosine or sine wave, but rather with a "wavelet," a particular pattern of oscillation that is localized in time or space. By moving the wavelet through the signal, analyzing the components of frequency as it goes, wavelet analysis can quantify when or where each frequency component contributes. Unfortunately, while there are a host of upper-level texts dealing with wavelets, I know of no truly introductory text.

And finally, I would be remiss if I didn't mention the use of sequential data in making predictions. In this chapter, we have focused on the analysis of measurements already in hand, but the pattern of variation measured in the past can be a potent guide to what will happen in the future. In spatial terms, the pattern of variation in one small part of the world can provide important information about patterns in adjacent areas. The use of sequential data to make predictions falls into the realm of *state-space modeling*, of which *Kalman filtering* is a particularly useful tool. Unfortunately, this type of analysis is well beyond the purview of this text, and I refer you to Priestley (1981) for an introduction.